Limnol. Oceanogr., 55(5), 2010, 2025–2036
© 2010, by the American Society of Limnology and Oceanography, Inc.
doi:10.4319/lo.2010.55.5.2025

Characterizing a cyanobacterial bloom in western Lake Erie using satellite imagery and meteorological data

Timothy T. Wynne,*[,a] Richard P. Stumpf,[a] Michelle C. Tomlinson,[a] and Julianne Dyble[b]

[a] National Oceanic and Atmospheric Administration, Center for Coastal Monitoring and Assessment, Silver Spring, Maryland
[b] National Oceanic and Atmospheric Administration, Great Lakes Environmental Research Laboratory, Ann Arbor, Michigan

Abstract

The distribution and intensity of a bloom of the toxic cyanobacterium, *Microcystis aeruginosa*, in western Lake Erie was characterized using a combination of satellite ocean-color imagery, field data, and meteorological observations. The bloom was first identified by satellite on 14 August 2008 and persisted for > 2 months. The distribution and intensity of the bloom was estimated using a satellite algorithm that is sensitive to near-surface concentrations of *M. aeruginosa*. Increases in both area and intensity were most pronounced for wind stress < 0.05 Pa. Area increased while intensity did not change for wind stresses of 0.05–0.1 Pa, and both decreased for wind stress > 0.1 Pa. The recovery in intensity at the surface after strong wind events indicated that high wind stress mixed the bloom through the water column and that it returned to the surface once mixing stopped. This interaction is consistent with the understanding of the buoyancy of these blooms. Cloud cover (reduced light) may have a weak influence on intensity during calm conditions. While water temperature remained > 15°C, the bloom intensified if there were calm conditions. For water temperature < 15°C, the bloom subsided under similar conditions. As a result, wind stress needs to be considered when interpreting satellite imagery of these blooms.

Toxic cyanobacterial blooms occur worldwide, on every continent except Antarctica (Carmichael 1992). These blooms are associated with detrimental effects, including human respiratory irritation, taste and odor of potable water, and human illness as a result of ingestion or skin exposure during recreation. Mortalities have been observed in domestic and wild animals (Hawkins et al. 1985; Carmichael 1998; Kuiper-Goodman et al. 1999). Additionally, cyanobacterial blooms can be aesthetically unappealing. This fact is amplified by a bloom's tendency to linger and become more concentrated along shorelines and in harbors where they are encountered more frequently by the public (Ibelings et al. 2003). It has been theorized that the presence, increase, and persistence of cyanobacterial blooms may also be a consequence of climate change and the resulting increase in water temperature (Paerl and Huisman 2008).

In the Great Lakes, the dominant toxic cyanobacterial genus is *Microcystis*, a highly buoyant colony-former that creates dense surface 'scums' in calm conditions. Historically, cyanobacterial blooms were an indicator of nutrient enrichment in shallow stratified areas of the Great Lakes in the 1960s and 1970s. While phosphorus reduction strategies decreased cyanobacterial biomass during the late 1980s and early 1990s, *Microcystis aeruginosa* blooms have resurged since 1995 and have appeared consistently each summer since then (Brittain et al. 2000; Vanderploeg et al. 2001). The large recurrence of *M. aeruginosa* blooms may be in response to the introduction of invasive zebra mussels of the genus *Dreissena*, which increased water clarity through filter feeding while selectively preying on eukaryotic phytoplankton, as opposed to cyanobacteria (Budd et al. 2001; Juhel et al. 2006).

* Corresponding author: Timothy.Wynne@noaa.gov

The most common phytoplankton groups found in western Lake Erie are chlorophytes, bacillariophytes, and cyanobacteria, together often comprising up to 90% of the total chlorophyll *a* (Chl *a*; Millie et al. 2009). Chlorophytes can make up to 50% of the phytoplankton Chl *a*, diatoms as high as 40%, and cyanobacteria between 10% and 30%. The dominant cyanobacterium is generally *Microcystis aeruginosa* in western Lake Erie, contributing 1–4% of the relative cyanobacterial biomass at the onset of a bloom, but increasing up to 99% at the height of a bloom (Millie et al. 2009; Rinta-Kanto et al. 2009). The exception is in Sandusky Bay, where up to 90% of the cyanobacterial biomass can be comprised of *Planktothrix agardii* (Fig. 1). These 2 cyanobacterial genera tend to dominate the phytoplankton community during the late summer.

Cyanobacterial blooms develop in warm, stratified water columns, with low winds and high light availability (Sellner 1997; Carmichael 2008; Paerl and Huisman 2008). They are relatively slow growing, with doubling periods on the order of 7 d (Fahnensteil et al. 2008). Intense surface concentration of cyanobacterial blooms may occur because of their positive buoyancy (Paerl 1988; Sellner 1997). Water temperatures above 15°C have been suggested as a contributing factor to the growth and senescence of cyanobacterial blooms. McQueen and Lean (1987) stated that cyanobacterial dominance generally occurs when water temperatures exceed 20°C. Robarts and Zohary (1987) show that *M. aeruginosa* populations expand in water temperatures between 15°C and 25°C. Wind speed, with a threshold of 4 m s^{-1}, has been suggested as a possible influence on the intensity of the bloom by changing its vertical distribution (Hunter et al. 2008). Strong winds mix the cells through the water column. During periods of weak winds, cyanobacteria may float to the surface, sometimes accumulating in high enough concentrations to form scums. Further examination of cyanobacterial blooms' response to these factors is

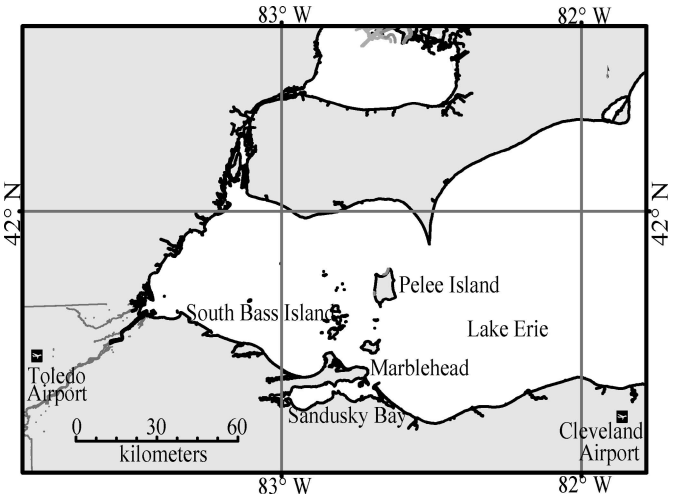

Fig. 1. A map showing points of interest within the study area.

necessary to understand and predict their distribution and intensity.

There have been several attempts to monitor and delineate cyanobacterial blooms using remotely sensed data (Kahru 1997; Simis et al. 2005; Ruiz-Verdú et al. 2008). The most common monitoring has been done on intense scum-forming blooms. Imagery from the Landsat and the Advanced Very High Resolution Radiometer (AVHRR) sensors have been suggested for detection of these types of cyanobacterial blooms (Kahru 1997; Vincent et al. 2004). The algorithms using these sensors may be unable to discriminate cyanobacterial blooms in areas with significant presence of noncyanobacterial material. This is due to the absence of a band targeting an optical signal that is able to discriminate cyanobacteria from other material. Additionally, the Landsat sensor (16-d repeat) lacks the temporal frequency for bloom monitoring. Kahru et al. (1997) have used data from the AVHRR to detect cyanobacterial blooms in the Baltic Sea. Although the AVHRR does have the temporal resolution to monitor blooms, this algorithm depends on water brightness. Although suitable for the scum-forming blooms in the Baltic, it is not effective for discrimination of cyanobacterial blooms in areas with plumes of sediment or other intense phytoplankton blooms (Kutser 2004).

Not all cyanobacterial blooms accumulate on the surface as scums, and algorithms have been developed that can identify or quantify blooms in the water column. A key algorithm proposed for estimating cyanobacteria from satellite was presented by Simis et al. (2005, 2007). They proposed a ratio algorithm using the 709-nm and 620-nm bands of the Medium Resolution Imaging Spectrometer (MERIS) on the Envisat satellite operated by the European Space Agency. They achieved very good results for sites in Spain and the Netherlands.

However, a potential problem with ratio-based remotely sensed algorithms is the relatively high frequency of atmospheric correction issues with MERIS level-2 data, leading to negative reflectance values in case-2 waters, causing algorithmic failure. The shape algorithm used here, and proposed by Wynne et al. (2008), will not be subjected to these failures, because this type of algorithm can accommodate negative reflectance values (Stumpf and Werdell 2010). This is due to the algorithm using a three-band shape, as opposed to a ratio, which would be exceedingly sensitive to a negative reflectance value. An advantage to using a three-band algorithm is that poorer quality imagery may still be used for interpretation. For example, pixels that may fail product-quality flags for atmospheric or glint correction may still be used. It should be noted that the algorithm used within this manuscript has not been statistically compared with previously published algorithms. The algorithm in this manuscript was tested using data from a 70-d period where in situ cell counts of *Microcystis aeruginosa* concentration ranged between 0 cells mL^{-1} and 1.6×10^7 cells mL^{-1}. This algorithm uses the spectral shape (or curvature) around 681 nm (*SS*(681)). A stronger curvature indicates higher concentrations of cyanobacteria (Wynne et al. 2008). These optical characteristics are consistent with the strong scattering by cyanobacteria, which cause elevated reflectance at 709 nm, (Gitelson 1992) therefore causing this algorithm to be potentially more sensitive to the optical characteristics possessed by *M. aeruginosa*, a small-celled cyanobacterium.

M. aeruginosa, contains gas vacuoles, and can vertically migrate through the water column. The buoyancy of the cells is governed by the production of carbohydrates through photosynthesis during sunlit hours. When a critical mass of carbohydrates accumulates in the cells, the cells tend to sink into the water column, and then begin utilizing these carbohydrates during respiration at night (Paerl and Huisman 2009). By morning most of the carbohydrates are molecularly degraded through respiration and the cells become buoyant and once again rise to the surface. MERIS makes its pass over the Great Lakes at $\sim$ 10:00 h Local Standard Time (Rast et al. 1999), by which time the cells should be within the first optical depth of the water during stratified conditions, hence making them detectable by satellite. Stratified conditions only occur in Lake Erie under low wind-stress conditions (Bolsenga and Herdendorf 1993; Millie et al. 2008, 2009).

In the summer of 2008, a large bloom of *M. aeruginosa* occurred in western Lake Erie, and persisted for $>$ 2 months. A satellite image time-series is presented here along with associated in situ observations (Fig. 2). A hypothesis is presented to explain the growth and cessation of the bloom, with an attempt to develop an ecological model to explain the development and demise of the bloom.

Methods

Remotely sensed data—Standard Reduced Resolution L2 satellite data from MERIS were acquired from the European Space Agency. Once the imagery was processed to normalized surface reflectance (*reflec*) using methods described by Montagner (2001), the cyanobacteria index (*CI*) was calculated following Wynne et al. (2008):

$$CI = -SS(681) \quad (1)$$

19395590, 2010, 5, Downloaded from https://aslopubs.onlinelibrary.wiley.com/doi/10.4319/lo.2010.55.5.2025 by Noaa Department Of Commerce, Wiley Online Library on [30/12/2024]. See the Terms and Conditions (https://onlinelibrary.wiley.com/terms-and-conditions) on Wiley Online Library for rules of use; OA articles are governed by the applicable Creative Commons License

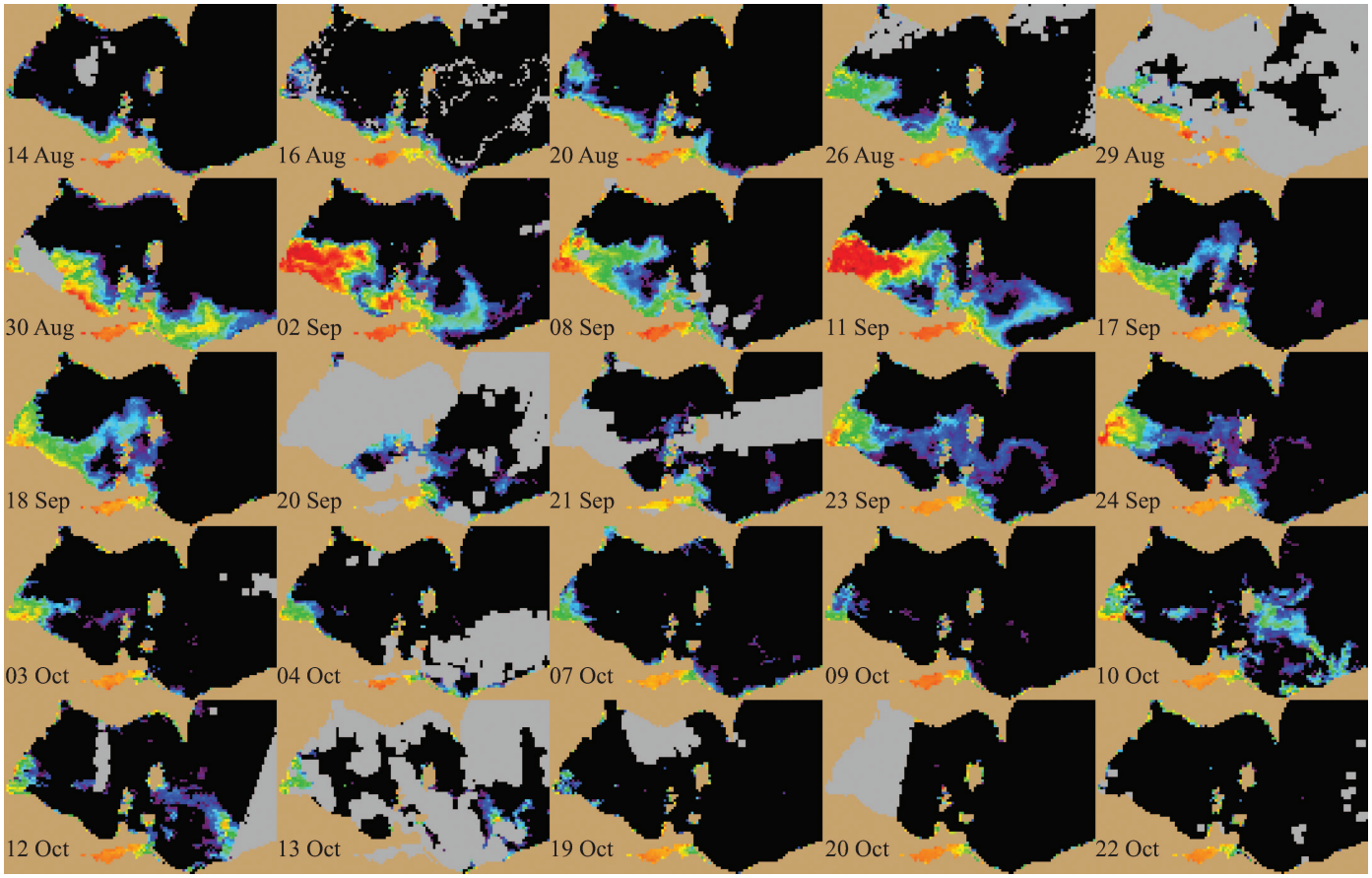

Fig. 2. A time series of MERIS-derived cyanobacterial index imagery from 2008. Black is indicative of pixels with a very low likelihood of a bloom, gray indicates clouds or missing data (off-nadir), and colored pixels are probable locations of cyanobacterial blooms. Warmer colors (red, orange, and yellow) are indicative of high concentrations of cyanobacteria and cooler colors (blue and purple) are indicative of low concentrations.

Where the spectral shape (or curvature) is determined as

$$SS(\lambda) = reflec(\lambda) - reflec(\lambda^-) - \{reflec(\lambda^+) - reflec(\lambda^-)\} \times \frac{(\lambda - \lambda^-)}{(\lambda^+ - \lambda^-)} \quad (2)$$

And λ = 681 nm (MERIS band 8), λ^+ = 709 nm (band 9), and λ^- = 665 nm (band 7).

This algorithm is an example of a shape algorithm described by Gower et al. (2005). A shape algorithm, such as that expressed in Eq. 2, reduces to the numerical second derivative when the bands are evenly spaced, such that $(\lambda^+ - \lambda) = (\lambda - \lambda^-$; Schowengerdt 1997; Wynne et al. 2008; Stumpf and Werdell 2010).

The Wynne et al. (2008) method uses a spectral shape, which (unlike ratio algorithms) is insensitive to the presence of negative radiances. Poor or incomplete atmospheric correction also does not influence the results, particularly as the bands are closely spaced. Gower et al. (2005) developed a similar spectral shape product called the Maximum Chlorophyll Index, using the top-of-atmosphere radiances from MERIS. The algorithm presented by Simis et al. (2005, 2007) is a semianalytic solution, which (although targeted toward phycocyanin) is subject to failure when used with poor-quality input water reflectance (e.g., negative). Negative reflectance on MERIS may result from inadequacies in either the atmospheric or glint corrections and their solution is beyond the scope of this study. As a result of the combination of conditions, the Wynne et al. (2008) method was applied to all data presented here. The time series shown in Fig. 2 had a varying amount of negative reflectance pixels recorded, ranging from 2% to 35% of the pixels that the Wynne et al. (2008) method derived as having an elevated Cyanobacterial Index, with the time-series average of 12.75%. Although it is true that various confidence flags may have been turned on in the L2 imagery used, the resultant images shown in Fig. 2 show no anomalous features, indicating that the algorithm used here may work just as effectively with lower quality imagery as it would with higher quality data.

A positive *CI* is indicative of elevated densities of cyanobacteria. The characteristics of the *CI* suggest that it will vary with concentration where a high *CI* is associated with higher density of cyanobacteria (Wynne et al. 2008). It should be noted that the algorithm employed here is not able to differentiate between different species of cyanobacteria. The algorithm may be sensitive to large blooms of

19395590, 2010, 5, Downloaded from https://aslopubs.onlinelibrary.wiley.com/doi/10.4319/lo.2010.55.5.2025 by Noaa Department Of Commerce, Wiley Online Library on [30/12/2024]. See the Terms and Conditions (https://onlinelibrary.wiley.com/terms-and-conditions) on Wiley Online Library for rules of use; OA articles are governed by the applicable Creative Commons License

other types of phytoplankton, which have the ability to effectively scatter light.

The *SS*(681) algorithm uses three bands in the red to near-infrared portion of the electromagnetic spectrum. The algorithm gives an estimate of cyanobacterial biomass in approximately one optical depth (Gordon and McCluney 1975). Gons et al. (2005) suggested that the optical depth of most inland waters that have problematic cyanobacterial blooms would be < 0.5 m. The mean specific absorption for phytoplankton in Lake Erie is 0.04 m^2 mg^{-1} chlorophyll (Binding et al. 2008). At 10 μg L^{-1} chlorophyll, an optical depth would be < 1 m at the 660–700-nm wavelengths, whereas pure water has an optical depth of ~ 2 m in these wavelengths (Pope and Fry 1997).

To quantify the concentration of cyanobacterial cells, the *CI* was summed for all available pixels in each image. This number was then normalized by the number of available bloom pixels ($n = 4288$) for analysis, where a bloom pixel is defined as a pixel that had a $CI > 0$ at some point during the 70-d time series presented within this manuscript (ignoring Sandusky Bay, which was flagged for cyanobacterial blooms throughout the time series). This normalized *CI* provides an estimate that can be used to derive the intensity of a cyanobacterial bloom for each image in the time series. In addition to the density, the normalized spatial extent (area) of the bloom was found by determining the area in each image that had a $CI > 0$. This number was then once again normalized by the number of bloom pixels available ($n = 4288$), where a bloom pixel was defined as a pixel that had a $CI > 0$ at some point during the 70-d time series shown in Fig. 2 (Fig. 3A).

Cell counts—Surface water samples were collected by grab sample from 10 to 12 stations throughout western Lake Erie on three separate dates corresponding to clear satellite imagery: 11 September, 24 September, and 07 October 2008. Samples for *Microcystis* spp. cell counts were preserved with 1% Lugols solution. Once in the laboratory, 10 mL of sample was gently filtered through a 1.2-μm Millipore filter, cleared by adding 50% gluteraldehyde, heated using a hot plate set to 60°C, dried overnight, and then mounted to a slide using Permount, according to Dozier and Richerson (1975). *Microcystis* colonies with cells of 3–5 μm in diameter (Komarek and Anagnostidis 1999) were counted. Measurements were made of the area of the colony, minus peripheral mucilage and empty interior spaces. From these values, biovolume and then equivalent spherical diameter (ESD) were calculated according to the methods of Hillebrand et al. (1999). From the colony ESD, cell number was calculated based on an empirical relationship derived from sonicating individual *Microcystis* colonies from western Lake Erie and enumerating cell numbers in those colonies (Dyble et al. 2008). Cell number was calculated as

$$\log Y = 2.83\ (\log_{10} X) - 2.50 \tag{3}$$

where Y is the cell number in cells mL^{-1} (Y), and X is the colony ESD. This method of cell counting has an error of 20% associated with it (Reynolds and Jaworski 1978).

Wind data—Hourly meteorological observations were downloaded from the National Oceanic and Atmospheric Administration (NOAA) National Data Buoy Center (NDBC) Sta. SBI01, located on South Bass Island, Ohio, U.S.A. (41.628 N 82.842 W; Fig. 1). Wind stress (τ) was calculated using

$$\tau = \rho \times C_D \times w^2 \tag{4}$$

where ρ is the density of air, estimated to be 1.25 kg m^{-3}, and C_D is the drag coefficient determined by (Hsu 1973):

$$C_D = 0.001 \times (0.69 + 0.081 \times w), \tag{5}$$

and w is the mean hourly wind speed.

An average wind stress was calculated by using the wind speeds from the 24 h preceding the time of a satellite image (Fig. 3B). Wind stress was used as it is expressed as a force, and a force is needed to drive the advective mixing needed to de-stratify the water column.

Water temperature—Water temperatures were obtained from the NOAA Center for Operational Products and Services (CO-OPS) Sta. 9063079, located at Marblehead, Ohio (41.545 N, 82.732 W). The 24-h mean water temperature was calculated from hourly observational data in the same fashion as for the winds (Fig. 3C).

Light availability (sun index)—To estimate light availability, the average sky cover between sunrise and sunset, reported in tenths of sky covered by clouds, was obtained from the National Weather Service for the Toledo Express Airport and Cleveland Hopkins International Airport (http://www.weather.gov/climate/index.php?wfo=cle). The National Weather Service reports 100% cloud-cover as 10 and clear conditions as 0. The inverse of this index was used for this study, because the desired value was the percentage of sun present and not the amount of clouds. The resultant index will be referred to as the 'sun index,' with a value of 10 indicating clear skies with 0% cloud cover, and a value of 0 indicating 100% cloud cover. The Toledo airport is to the west of the bloom area, and the Cleveland airport is to the southeast of the bloom area (Fig. 1). A mean was calculated using the two stations in an effort to try and estimate the sun conditions in the area around the bloom (Fig. 3D). It should be noted that the Toledo airport generally experienced clearer skies throughout the time series relative to the Cleveland airport.

Results

Field validation—Cell counts from 3 d (11 Sep, 24 Sep, and 03 Oct 08) were compared with the satellite derived *CI*. These cell counts were from same-day match-ups. Cyanobacterial blooms are extremely patchy at subpixel scales (Kutser et al. 2008). In the data collected for this study, two points were collected from one station (latitude 41.7919, longitude −83.3925) on 28 August (data not shown because no image was available for this date). The cell counts from these two samples varied in concentration by an order of magnitude (3.6×10^5–3.7×10^6 cells mL^{-1}), illustrating the

19395590, 2010, 5, Downloaded from https://aslopubs.onlinelibrary.wiley.com/doi/10.4319/lo.2010.55.5.2025 by Noaa Department Of Commerce, Wiley Online Library on [30/12/2024]. See the Terms and Conditions (https://onlinelibrary.wiley.com/terms-and-conditions) on Wiley Online Library for rules of use; OA articles are governed by the applicable Creative Commons License

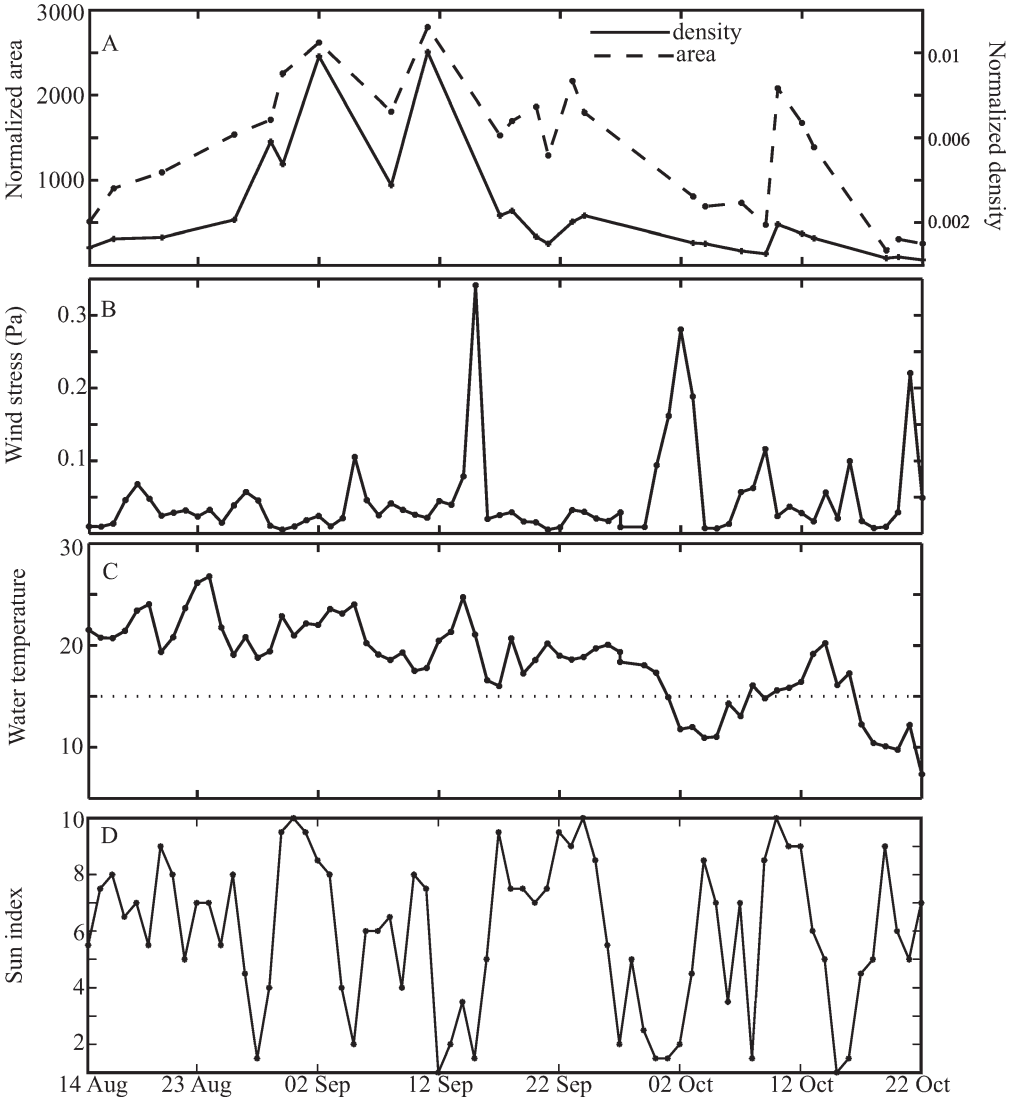

Fig. 3. Time series plots from 14 August to 22 October 2008. (A) Graph showing the normalized areal coverage of the bloom (dashed line) and the normalized density of the bloom (solid line). These data were extracted from the time series in Fig. 2. Note that the two lines closely follow each other in shape and magnitude until the large wind event on 15 September, after which the shapes are still similar but the density is much reduced. (B) Graph showing the mean daily wind stress from wind-speed data reported by NOAA's NDBC station at South Bass Island. (C) Graph showing the mean daily water temperature as reported by NOAA's CO-OPS station at Marblehead, Ohio, U.S.A. The dashed line shows the 15°C point mentioned in the text. (D) Graph showing the sun index, as reported by the National Weather Service. A score of 10 indicates a fully clear sky. A score of 0 indicates a fully cloudy sky. These data are a daily average of the hours between sunrise and sunset, and a mean of the conditions reported at the Toledo Airport and the Cleveland Airport.

patchiness of blooms. The resultant graph shows the correlation of *CI* to cell count (Fig. 4). Kutser (2004) noticed the same phenomenon, as he found chlorophyll concentrations ranging two orders of magnitude within the space of 1 km^2. While variability certainly exists, the trend is for increasing cell count with an increasing *CI*. Subramanium et al. (2002) noted bloom patchiness in oceanic cyanobacteria and questioned the validity of using SeaWiFS imagery to detect blooms. Kutser (2004) showed that 30-m satellite data (from Hyperion) can be inadequate for resolving the patchiness in blooms of cyanobacteria. Yacobi et al. (1995) noted that chlorophyll concentrations differed by 300% on different sides of a research vessel in a dinoflagellate bloom (dinoflagellates swim, leading to concentration patterns similar to buoyant cyanobacteria). Considering the natural variability that is present in the system, the data in Fig. 4 are reasonably correlated.

Binned cell counts were overlaid on three cloud-free images taken on the same day to examine consistency in the spatial patterns (Fig. 5). The first image, from 11 Septem-

19395590, 2010, 5, Downloaded from https://aslopubs.onlinelibrary.wiley.com/doi/10.4319/lo.2010.55.5.2025 by Noaa Department Of Commerce, Wiley Online Library on [30/12/2024]. See the Terms and Conditions (https://onlinelibrary.wiley.com/terms-and-conditions) on Wiley Online Library for rules of use; OA articles are governed by the applicable Creative Commons License

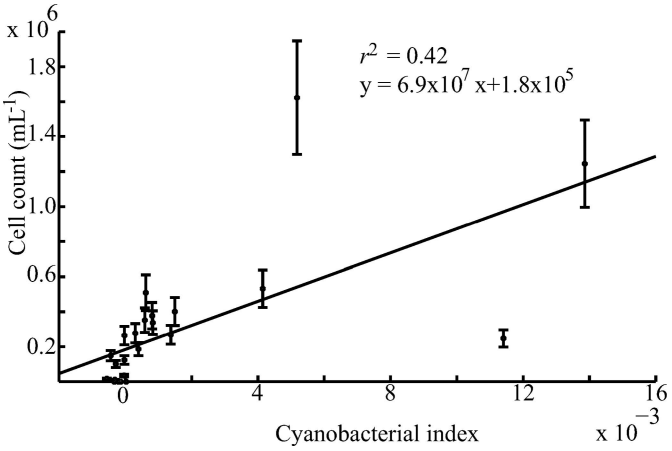

Fig. 4. A comparison between the derived cyanobacterial index (*CI*) and *Microcystis* cell counts (cells mL^{-1}). The error bars represent the 20% error encountered while performing cell counts.

ber, was the day of the highest biomass observed from satellite. The second image (24 Sep) followed the highest observed wind stress of the time series presented here, and the last image (07 Oct) was toward the end of the bloom; hence, these three images present a dynamic range of cyanobacterial biomass. Bins were made with cell counts and the *CI*. Absent corresponds to a $CI < 0$, and cell counts of 0; Low is a *CI* between 0 and 0.0004 and cell counts between 1 and 300,000 cells mL^{-1}, Medium has a $CI >$ 0.0004–0.004 and cell counts between 300,001 and 500,000 cell mL^{-1}, and High has a $CI > 0.004$, and cell counts $>$ 500,000 mL^{-1} (Fig. 5). The disagreements between the cell counts and the *CI* occur in areas where biological fronts are present and variability is high. To show the efficacy of this analysis, a producer's accuracy and user's accuracy was calculated (Story and Congalton 1986; Congalton 1991), and a summary of the comparisons are shown in Table 1. The user's accuracy is a measure of commission error, indicative of a probability that a pixel is properly classified into one of the given categories. The producer's accuracy measures omission error, indicative of the probability that a category is correctly classified to a pixel.

Bloom development—The bloom of interest was first observed in the satellite data on the southwest shore of Lake Erie on 14 August (Fig. 2). The bloom, according to satellite imagery, intensified for a period of several weeks, until 02 September (Fig. 3A). The time period between 14 August and 02 September, when the greatest intensification occurred, was characterized by warm water (temperatures between 19°C and 27°C; Fig. 3C). The light availability during this time was generally high, with an average sun index > 5 ($< 50\%$ cloud cover) for 16 out of the 19 d during this period (Fig. 3D). The sun index is defined in the Light Availability section of this manuscript. The wind stress was relatively low (< 0.07 Pa), particularly during the 4 d leading up to 02 September (0.02 Pa; Fig. 3B). Two perturbations are seen in the overall increase in the bloom intensity from 14 August to 02 September (Fig. 3A). The rate of increase was low from 16 August to 20 August, which included a 24-h wind stress of 0.07 Pa. The bloom intensity increased from 20 August to 02 September. There was a slight decrease in cyanobacterial concentration between 02 September and 08 September. On 05 September, a wind stress of 0.1 Pa was recorded, the highest yet in this time series. Following this high wind stress, the concentration and area of the near-surface bloom was reduced. The light availability levels were lower during this time as well, and may have also been a contributing factor to the apparent decrease in cyanobacterial concentrations. The bloom increased again from 08 to 11 September, when it reached its maximum concentration, according to satellite imagery. Water temperature was relatively constant over this 3-d period, with an ~ 1.0°C variation. The amount of light availability increased, because mostly clear skies were observed in the area for the 3-d period between 08 September and 11 September. The wind stress was relatively low throughout this time.

Bloom cessation—After 11 September, the bloom declined in a series of events. The first occurred from 11 to 17 September, the second from 23 September to 03 October, and the third after 12 October, with the bloom disappearing altogether by 22 October.

The 24-h period before the image taken on 14 September had an average wind speed exceeding 19 m s^{-1}, and led to the strongest wind stress observed during the duration of the bloom ($\tau > 0.34$ Pa). After this event, the estimated bloom area decreased from 40% to 25% of the cloud-free pixels and the apparent surface concentration also decreased to levels observed in early August. This was particularly the case in the eastern area of the bloom, east of South Bass Island, where the water is generally deeper than to the west of the island (12–15 m vs. 5–8 m; Great Lakes Atlas 1995). The strong wind event was accompanied by low light levels, because four straight days of cloudy to mostly cloudy conditions were present in the area between 12 September and 15 September. The water temperature varied between 25°C and 16°C.

Between 17 September and 23 September, the bloom was somewhat stable. It did reappear in the area east of South Bass Island, but not to the same intensity as early September. The second decrease in bloom intensity occurred from 23 September to 03 October. No bloom is evident east of S. Bass Island on 03 October. This period included a wind stress of the second highest level for the length of the time series (0.3 Pa) on 01 October. Between 28 September and 03 October, there also was a drop in water temperature, as temperatures went from 19°C to as low as 12°C. This is the first period in the time series that the water temperature fell below 15°C. There were also low light levels between 24 September and 03 October.

From 03 October until 09 October, the bloom experienced a gradual decrease in intensity and extent. Wind stress was between 0.05 and 1.0 Pa and water temperature was below 15°C. On 10 October, it appears that the eastern portion of the bloom (E of South Bass Island) resurfaced. The wind stress decreased from 0.1 Pa on 09 October to about 0.04 Pa on 10 October. Temperatures were above 15°C and the sun index was > 9 during this rebound. The

19395590, 2010, 5, Downloaded from https://aslopubs.onlinelibrary.wiley.com/doi/10.4319/lo.2010.55.5.2025 by Noaa Department Of Commerce, Wiley Online Library on [30/12/2024]. See the Terms and Conditions (https://onlinelibrary.wiley.com/terms-and-conditions) on Wiley Online Library for rules of use; OA articles are governed by the applicable Creative Commons License

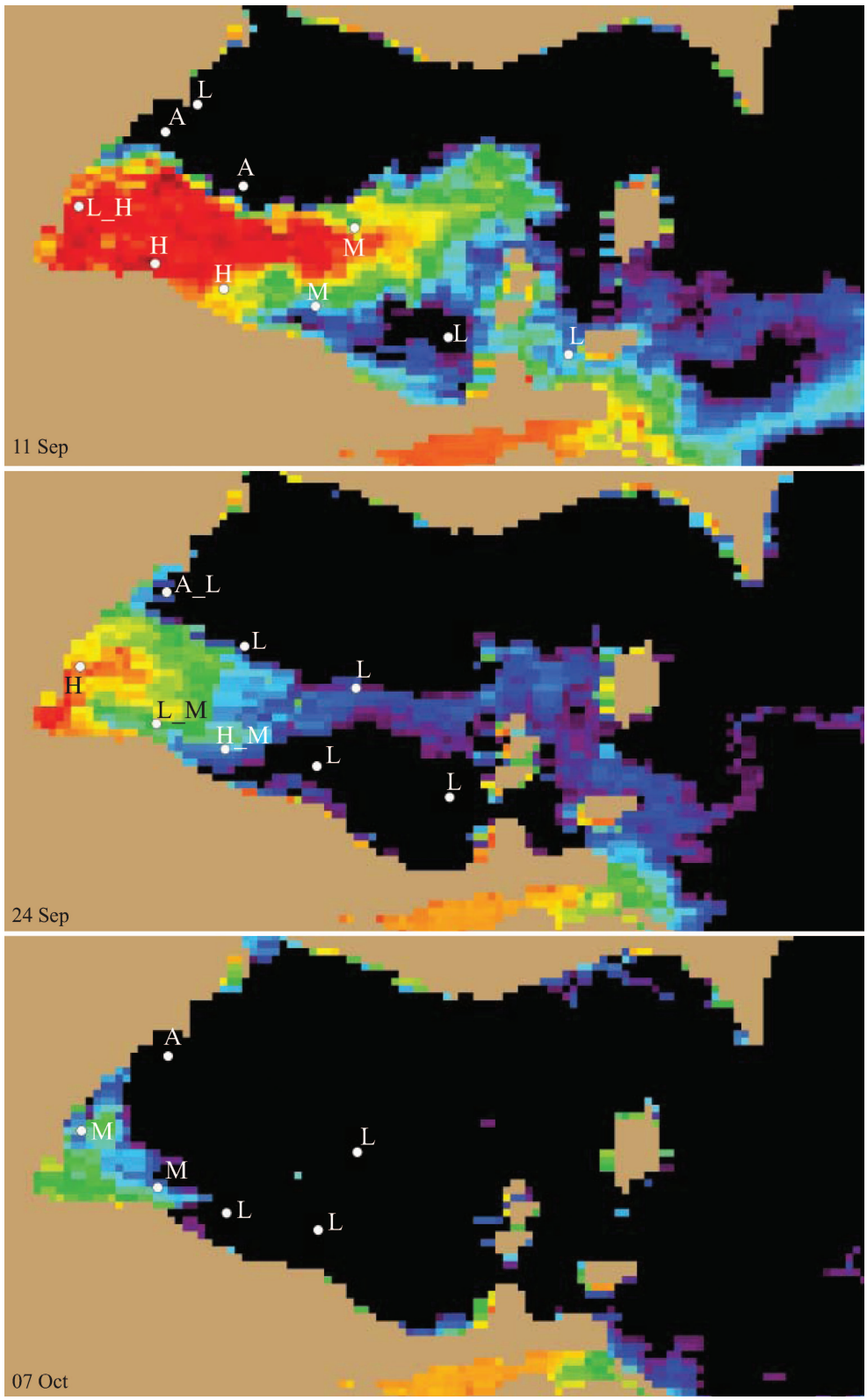

Fig. 5. *Microcystis* cell counts overlaid on the cyanobacterial index image. 'A' signifies the absence of a cell count or a positive *CI*. 'L' signifies a low threshold (*CI* 0–0.0004; cell count 1–300,000 cells L^{-1}). 'M' signifies a medium threshold ($CI > 0.0004$–0.004; cell counts 300,001–500,000 cells L^{-1}). 'H' signifies a high threshold ($CI > 0.004$; cells > 500,000 cells L^{-1}). When more than one letter is present, the first refers to the cell count and the second refers to the *CI*, when only one letter is present cell count and *CI* is in agreement.

19395590, 2010, 5, Downloaded from https://aslopubs.onlinelibrary.wiley.com/doi/10.4319/lo.2010.55.5.2025 by Noaa Department Of Commerce, Wiley Online Library on [30/12/2024]. See the Terms and Conditions (https://onlinelibrary.wiley.com/terms-and-conditions) on Wiley Online Library for rules of use; OA articles are governed by the applicable Creative Commons License

Table 1. Accuracy of binned cell counts with binned *CI*.

Index/cells	High	Medium	Low	Absent	Raw total	% user's accuracy
High	3	0	1	0	4	75
Medium	1	4	1	0	6	67
Low	0	0	10	1	11	91
Absent	0	0	0	3	3	100
Column total	4	4	12	4	24	—
% producer's accuracy	75	100	83	75	—	—

eastern bloom was visible from 10 to 13 October. This corresponds to a time when the wind stress was low and the temperature remained above 15°C.

The last event after 12 October resulted in the disappearance of the bloom by 22 October. The intervening time had a wind event of 0.1 Pa, with water temperatures below 11°C and low sun index. The western portion of the bloom, near the mouth of the Maumee River, decreased from 10 to 19 October and was no longer visible on or after 22 October.

Discussion

The MERIS satellite imagery, in combination with the physical data presented here of wind stress, water temperature, and light availability, was effective in characterizing the *Microcystis* bloom in western Lake Erie during the summer and autumn of 2008.

Wind—The decreases in bloom area and intensity occurred after daily wind stresses exceeded 0.1 Pa (equating to a wind speed of $\sim$ 7.7 m s^{-1}). This is generally higher then observations made by George and Edwards (1976), who noted that wind speeds in excess of 4 m s^{-1} (0.02 Pa) were sufficient to cause buoyant cyanobacteria to be submerged below the surface. Hunter et al. (2008) noted that the blooms of *M. aeruginosa* were driven to depth by wind speeds of 6 m s^{-1} (0.053 Pa). It should be noted that in both of these examples the water bodies under consideration were small and shallow relative to the western basin of Lake Erie. The lake that Hunter et al. (2008) examined (Barton Broad, U.K.) had an average depth of 1.2 m. Because western Lake Erie is much deeper ($\sim$ 5–15 m), it would be expected that a stronger wind stress would be required to mix the bloom through the water column, because generally deeper water will be more stratified and require a greater stress for mixing. Western Lake Erie may have a modest thermocline, which must be overcome for cells to be mixed throughout the water column.

A wind event of 0.1 Pa appears consistent with a mixing event that is strong enough to submerge the cells to reduced or even undetectable levels (from satellite) in Lake Erie. The trend can be seen throughout the time series where the wind stress exceeded 0.1 Pa. For example, a decrease in bloom area and concentration occurred after the strongest wind event of the observed period (0.34 Pa on 15 Sep). The bloom never fully recovered after this point, which may have partially been due to reduced light availability at depth and decreasing temperature, as described below. The water may have not fully restratified after this event, thereby allowing smaller wind stresses the ability to mix the cells homogeneously through the water and not allowing remote detection.

Conversely, in late August, the normalized area and density tended to increase during periods of low wind stress ($<$ 0.05 Pa). Wind stress between 0.05 and 0.1 Pa appeared to slow this intensification. This probably results from partial mixing of the bloom into the water column resulting in a real decrease in surface concentration, and an apparent decrease in bloom area.

Gons et al. (2005) made note that the near-surface concentration of *Microcystis* will be higher during periods of low wind stress, and that during periods of high wind stress, the cells will be homogeneously mixed throughout the water column. It appears that the same factors are applied to the case of this bloom. The satellite may give an accurate representation of the biomass during mixed conditions provided that the bathymetry is accounted for (Wynne et al. 2006). However, without knowledge of the vertical distribution of the cells it will be impossible to determine this.

Temperature—Water temperature has been hypothesized as a key factor in the growth and cessation of cyanobacterial blooms (Paerl 1988; Sellner 1997; Paerl and Huisman 2008). In this study, rapid expansion and intensification of the bloom occurred during a period with water temperature $>$ 19°C. On 01 October, the temperature fell below the threshold for algal bloom development of 15°C proposed by Robarts and Zohary (1987) for the first time in the considered time series. The combination of temperature and wind appeared to weaken the bloom. There was recovery of the areal coverage of the bloom, but not of bloom intensity (Fig. 3A). After 13 October, the bloom did not recover despite low wind stress. A series of high wind-stress events (09, 16, and 21 Oct) and temperatures below 15°C may have prevented the recovery of the bloom, even during periods of low wind stress, eventually leading to bloom cessation.

Light—Light availability may play a slight role in the formation and cessation of blooms; however, any influence is obscured by the association of bloom density with wind stress and water temperature during the study period discussed here. This may change as a function of season. Generally, the bloom described in this manuscript grew with clearer skies and subsided with cloudier skies. This may be due to confounding factors. Clear sunny skies were

19395590, 2010, 5, Downloaded from https://aslopubs.onlinelibrary.wiley.com/doi/10.4319/lo.2010.55.5.2025 by Noaa Department Of Commerce, Wiley Online Library on [30/12/2024]. See the Terms and Conditions (https://onlinelibrary.wiley.com/terms-and-conditions) on Wiley Online Library for rules of use; OA articles are governed by the applicable Creative Commons License

Table 2. Hypothesized rule-based model for estimating cyanobacterial bloom presence and intensity, when temperature >15°C.

Wind stress (Pa)	Duration	Bloom response	Satellite near-surface biomass estimate
<0.05	>5 d	bloom growth bloom at surface	accurate near-surface
<0.05	1 d	bloom moving to surface	underestimate
0.05–0.1	1 d	partial mixing	underestimate
>0.1	1 d	complete mixing	severe underestimate or failure
<0.05	>5 d	no growth bloom at surface	accurate near-surface
<0.05	1 d	bloom moving to surface	underestimate
0.05–0.1	1 d	partial mixing	underestimate
>0.1	1 d	complete mixing	severe underestimate

accompanied by periods of low wind stress and warm water temperatures, and periods of cloudy skies were accompanied by periods of high wind stress. It is possible that the light is the driving factor to the reduction in cyanobacterial bloom intensity. However, the hypothesis presented here indicates that the wind stress is the driving factor and reduction in bloom intensity on satellite imagery is due to the bloom being mixed through the water column, thereby reducing the concentration in the first optical depth (upper 1 m). The data presented in the time series in Fig. 3 support this hypothesis. Comparing the Sun Index with bloom area and extent (Fig. 3A) shows some mismatches. On 28 August the sun index is reported as 1, (90% clouds), which had no apparent adverse effect on the concentration of bloom-forming cells or area. The same trend is seen at the end of the time series, when 19 October, a clear day with little wind, had no positive effect on the concentration or extent of the bloom.

Interpretations of observations—The use of satellite imagery to observe cyanobacterial blooms is hypothesized to be modulated by wind and temperature conditions (Table 2). In using satellite imagery to characterize cyanobacterial bloom intensity, wind stress is hypothesized as the dominant factor, but is modulated by the water temperature. Wind stress may provide a potential indicator to describe how the bloom is distributed through the water column. Under weak wind there will not be the needed turbulence to mix the cells, thereby allowing them to congregate at the surface. Thus, the satellite should be able to deliver a more accurate representation of the areal biomass (Gons et al. 2005; Hunter et al. 2008). During high wind-stress conditions, satellite imagery will provide near-surface (< 1 m) concentrations. However, the total areal biomass of the bloom will be underestimated because the cells will be mixed throughout the water column.

To further show the efficacy of the wind-mixing hypothesis, an analysis was performed using the 11 September and 17 September imagery. If we assumed first, that the bloom was concentrated uniformly in the upper 1 m of water on 11 September, and second that mixing dispersed the bloom uniformly through the water column on 17 September, then the *CI* on 11 September divided by the water depth should equal the *CI* on 17 September (Fig. 6). Water depth was obtained from the NOAA Geophysical Data Center's bathymetry data. The transect follows a zone where both 11 September and 17 September had measurable *CI*s. The high correlation ($r^2 = 0.76$) and slope of near unity (0.95) indicate that the bloom was not reduced, but rather was mixed through the water column. This analysis makes two basic assumptions. The first assumption is that the bloom did not grow significantly over this relatively short time period, which is plausible as *Microcystis* spp. has a growth rate on the order of 0.1 d^{-1} in the Great Lakes (Fahnenstiel et al. 2008). The second assumption is that the optical depth would have remained < 1 m on both days.

It is hypothesized that during periods of wind stress > 0.1 Pa, it can be assumed that the use of *CI* will be less effective in delineating the bloom, because the near-surface

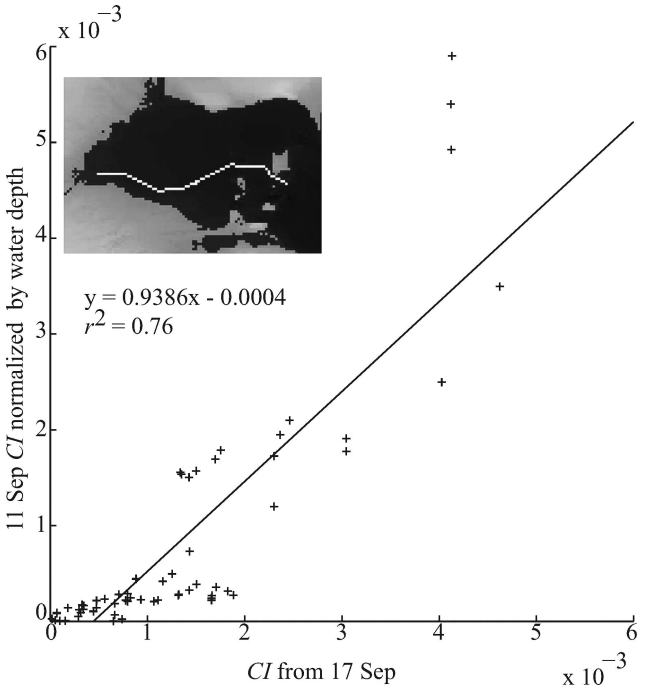

Fig. 6. Correlation between the *CI* concentration from 17 September and the depth-integrated *CI* concentration from 11 September. This tight correlation supports the hypothesis that the cyanobacterial bloom was relatively homogeneously mixed through the water column by the strong mixing event from 15 September. The data presented in the graph were extracted from the transect shown in the embedded image.

19395590, 2010, 5, Downloaded from https://aslopubs.onlinelibrary.wiley.com/doi/10.4319/lo.2010.55.5.2025 by Noaa Department Of Commerce, Wiley Online Library on [30/12/2024]. See the Terms and Conditions (https://onlinelibrary.wiley.com/terms-and-conditions) on Wiley Online Library for rules of use; OA articles are governed by the applicable Creative Commons License

concentration is below the sensitivity of remotely sensed methods. With water temperatures remaining compatible with cyanobacterial preferences from September 11 to September 17, it is unlikely that water temperature played a significant role in perceived short-term gains and losses in the surface manifestation of the bloom. It does appear, from the data presented here, that when the water temperature drops below 15°C the bloom rapidly dissipates.

Can other factors explain the observed variations? These factors would be introduced either through mortality or growth of the cyanobacterial cells. If the wind increased mixing, it could potentially also introduce new nutrients, which could cause growth. Cyanobacteria are slow growing, with growth rates of 0.1 d^{-1} (Fahnenstiel et al. 2008), this is equivalent to saying it would take $\sim$ 7 d for the cyanobacterial biomass to double. Growth would explain the initial increase in *CI* from 14 August to 02 September, under calm conditions, a four-fold increase in *CI* over the span of 19 d would be expected (assuming a growth rate of 0.1 d^{-1}). This growth was probably caused by the initial nutrient supply. However, the subsequent increases in biomass of two to three-fold over a few days is faster than can be explained by growth. The decline at the end of the season may be caused by nutrient exhaustion rather than temperature stress. Although the results are consistent with temperature, this study cannot discount nutrient loss as a possible cause for bloom cessation.

This result leads to a model for improving interpretation of the satellite imagery. It allows for the possibility of estimating surface and near-bottom concentrations of cyanobacteria using a rule-based approach (Table 2). If the wind stress is $>$ 0.1 Pa, it is hypothesized that the cyanobacterial biomass is roughly homogeneously distributed throughout the water column, and multiplying the *CI* by the mixing depth would yield an approximation of the areal biomass. If the wind stress is $<$ 0.05 it is hypothesized that the cyanobacterial biomass is congregated near the surface and a remotely sensed estimate would be a reasonable approximation of areal biomass. If the wind stress is between 0.05 and 0.1 Pa, the bloom is partially mixed and the biomass would be more than that recorded by satellite but less than the product of the *CI* and the bathymetry. These techniques will have some limitations, such as when the cells form a surface scum, when the cyanobacteria are present within a mixed bloom with other nonbuoyant phytoplankton, or in water where windstress is unable to mix through a well-established thermocline. Use of rigorous mixing models would be an appropriate next step in examining blooms dominated by buoyant cyanobacteria.

The interaction of physical forcing with bloom intensity was also studied. There are other factors that are important in determining the growth of cyanobacterial blooms (Millie et al. 2009) that were beyond the scope of this study. Nutrient loads from the watershed, particularly through the Maumee and Sandusky Rivers, are critical to initiating and promoting bloom growth in western Lake Erie. No nutrient data were available for this study and nutrient fluxes were not considered as a potential factor to enhance the growth or cessation of the bloom presented here. There have been a number of studies done that have considered the effects of nutrients on the growth and cessation of *Microcystis*. This study considered very short time periods over the course of a longer 70-d series. Considering the slow growth rates of *Microcystis* (0.1 d^{-1} [Fahnenstiel et al. 2008]) the nutrient flux would most likely play a reduced role in bloom cessation and growth relative to physical processes over the span of $<$ 5 d. Further developments of ecological models for the prediction of *Microcystis* blooms in western Lake Erie would also need to consider nutrient loading through the watershed and internal loading from sediments.

Management Implications

M. aeruginosa blooms pose a potential risk for recreational and potable water supplies. The environmental characteristics of the risk are different for each water source. High concentrations near the surface are the primary risk for recreational activities, such as swimming and boating. Concentrations near the bottom of the water column pose a risk for potable water supply, because intakes may be located near there. Identifying surface blooms during calm conditions clearly aids in monitoring for recreation. By combining this information with wind stress, inference can be made of the vertical distribution of cyanobacteria. For example, the bloom of 11 September was mixed into the water column by the 15 September wind event. Using the 17 September image alone would lead to an underestimation of the presence and potential risk of the bloom. Using the 11 September image with the wind-stress information (Table 2) would allow an estimate of near-bottom concentrations. Similar estimates could be made for 17 September. Recovery appears to take $\sim$ 5 d of $<$ 0.05-Pa winds. The duration of recovery is dependent on the depth of the lake. In the case of Hunter et al. (2008), changes required only hours in a lake with a maximum depth of $<$ 2 m.

In conclusion, the ability to monitor and forecast cyanobacterial blooms with satellite imagery (or satellite-derived data) would be a substantial contribution to the fields of both ecology and public health. The detection algorithm presented here appears to be satisfactory in delineating the extent and surface concentration of a cyanobacterial bloom in western Lake Erie. Using a simple rule-based model that combines the satellite algorithms with environmental and meteorological observations, it is hypothesized that it is possible to determine the distribution of a bloom through the water column and whether the bloom may intensify or diminish, assuming that factors not available from remote observations, such as nutrient supply and mortality, remain constant. This may lead to predictive capabilities for cyanobacterial blooms.

Acknowledgments

Medium Resolution Imaging Spectrometer Instrument (MERIS) imagery was provided by the European Space Agency (Category-1 Proposal C1P.3975). Lee Wyrobek and Sander Robinson contributed to the field sampling and processing. Travis Briggs provided various contributions to this submission. We thank two anonymous reviewers whose comments greatly strengthened this paper. Funding was provided by the National

19395590, 2010, 5, Downloaded from https://aslopubs.onlinelibrary.wiley.com/doi/10.4319/lo.2010.55.5.2025 by Noaa Department Of Commerce, Wiley Online Library on [30/12/2024]. See the Terms and Conditions (https://onlinelibrary.wiley.com/terms-and-conditions) on Wiley Online Library for rules of use; OA articles are governed by the applicable Creative Commons License

Oceanic and Atmospheric Administration's (NOAA) Center of Excellence for Great Lakes and Human Health, and through the National Center for Environmental Health at the Centers for Disease Control and Prevention and by the NASA Applied Science Program announcement NNH08ZDA001N under contract NNH09AL53I.

References

Binding, C. E., J. H. Jerome, R. P. Bukata, and W. G. Booty. 2008. Spectral absorption of dissolved and particulate matter in Lake Erie. Remote Sens. Environ. **112:** 1702–1711.

Bolsenga, S. J., and C. E. Herdendorf. 1993. Lake Erie and Lake St. Claire handbook. Wayne State Univ. Press.

Brittain, S. M., J. Wang, L. Babcock-Jackson, W. W. Carmichael, K. L. Rinehart, and D. A. Culver. 2000. Isolation and characterization of microcystins, cyclic hepatotoxins from Lake Erie strains of *Microcystis aeruginosa*. J. Gt. Lakes Res. **26:** 241–249, doi:10.1016/S0380-1330(00)70690-3

Budd, J. W., T. D. Drummer, T. F. Nalepa, and G. L. Fahnenstiel. 2001. Remote sensing of biotic effects: Zebra mussels (*Dreissena polymorpha*) influence on water clarity in Saginaw Bay, Lake Huron. Limnol. Oceanogr. **46:** 213–223.

Carmichael, W. W. 1992. A status report on planktonic cyanobacteria (blue green algae) and their toxins. U.S. Environmental Protection Agency, Environmental Monitoring Systems Laboratory, Office of Research and Development.

———. 1998. Algal poisoning, p. 2022–2023. *In* S. Aiello [ed.], The Merck veterinary manual. Merck.

———. 2008. A world overview one-hundred, twenty-seven years of research on toxic cyanobacteria—where do we go from here? Adv. Exp. Med. Biol. **619:** 105–125, doi:10.1007/978-0-387-75865-7_4

Congalton, R. G. 1991. A review of Assessing the accuracy of classifications of remotely sensed data. Remote Sens. Environ. **37:** 35–46, doi:10.1016/0034-4257(91)90048-B

Dozier, B. J., and P. J. Richerson. 1975. An improved membrane filter method for the enumeration of phytoplankton. Verh. Int. Ver. Limnol. **19:** 1524–1529.

Dyble, J., G. L. Fahnenstiel, R. W. Litaker, D. F. Millie, and P. A. Tester. 2008. Microcystin concentrations and genetic diversity of *Microcystis* in the lower Great Lakes. Environ. Toxicol. **23:** 507–516, doi:10.1002/tox.20370

Fahnenstiel, G. L., and others. 2008. Factors affecting microcystin concentration and cell quota in Saginaw Bay, Lake Huron. Aquat. Ecosyst. Health Manag. **11:** 190–195, doi:10.1080/14634980802092757

George, D. G., and R. W. Edwards. 1976. The effect of wind on the distribution of chlorophyll-*a* and crustacean plankton in a shallow eutrophic reservoir. J. Appl. Ecol. **13:** 667–690, doi:10.2307/2402246

Gitelson, A. 1992. The peak near 700 nm on radiance spectra of algae and water: Relationships of its magnitude and position with chlorophyll concentration. Int. J. Remote Sens. **13:** 3367–3373, doi:10.1080/01431169208904125

Gons, H. J., H. Hakvoort, S. W. M. Peters, and S. G. H. Simis. 2005. Optical detection of cyanobacterial blooms, p. 177–199. *In* J. Huisman, H. C. P. Matthijs and P. M. Visser [eds.], Harmful cyanobacterial. Springer.

Gordon, H. R., and W. R. McCluney. 1975. Estimation of the depth of sunlight penetration in the sea for remote-sensing. Appl. Optics **14:** 413–416, doi:10.1364/AO.14.000413

Gower, J., S. King, G. Borstad, and L. Brown. 2005. Detection of intense plankton blooms using the 709nm band of the MERIS imaging spectrometer. Int. J. Remote Sens. **26:** 2005–2021, doi:10.1080/01431160500075857

Great Lakes Atlas. 1995. Jointly produced by the Government of Canada and U.S. Environmental Protection Agency [accessed 24 July 2008]. Available online at: http://www.epa.gov/glnpo/atlas/index.html.

Hawkins, P. R., M. T. C. Runnegar, A. R. B. Jackson, and I. R. Falconer. 1985. Severe heptatoxicity caused by the tropical cyanobacterium (blue-green alga) *Cylindrospermopsis raciborskii* (Woloszynska). Seenayya and Subba Raju isolated from a domestic water supply reservoir. Appl. Environ. Microb. **50:** 1292–1295.

Hillebrand, H., C. D. Durselen, D. Kirschtel, U. Pollingher, and T. Zohary. 1999. Biovolume calculation for pelagic and benthic microalgae. J. Phycol. **35:** 403–424, doi:10.1046/j.1529-8817.1999.3520403.x

Hsu, S. A. 1973. Experimental results of the drag-coefficient estimation for air–coast interfaces. Bound.-Lay. Meteorol. **6:** 505–507, doi:10.1007/BF02137682

Hunter, P. D., A. N. Tyler, N. J. Willby, and D. J. Gilvear. 2008. The spatial dynamics of vertical migration by *Microcystis aeruginosa* in a eutrophic shallow lake: A case study using high spatial resolution time-series airborne remote sensing. Limnol. Oceanogr. **53:** 2391–2406.

Ibelings, B. W., M. Vonk, H. F. J. Los, D. T. Van der Molen, and W. M. Mooij. 2003. Fuzzy modeling of cyanobacterial surface waterblooms: Validation with NOAA-AVHRR satellite images. Ecol. Appl. **13:** 1456–1472, doi:10.1890/01-5345

Juhel, G., and others. 2006. Pseudodiarrhoea in zebra mussels *Dreissena polymorpha* (Pallas) exposed to microcystins. J. Exp. Biol. **209:** 810–816, doi:10.1242/jeb.02081

Kahru, M. 1997. Using satellites to monitor large-scale environmental change in the Baltic Sea, p. 43–61. *In* M. Kahru and C. W. Brown [eds.], Monitoring algal blooms: New techniques for detecting large-scale environmental change. Springer-Verlag.

Komarek, J., and K. Anagnostidis. 1999. Cyanoprokaryota: Teil chroococcales, p. 1–548. *In* A. Pasher, H. Ettl, G. Gartner, H. Heynig and D. Mollenhauer [eds.], Subwasserflora von Milleleuropa. Gustay Fischer.

Kuiper-Goodman, T., I. R. Falconer, and J. Fitzgerald. 1999. Human health aspects, p. 113–153. *In* I. Chorus and J. Bartram [eds.], Toxic cyanobacteria in water. A guide to their public health consequences, monitoring and management. World Health Organization.

Kutser, T. 2004. Quantitative detection of chlorophyll in cyanobacterial blooms by satellite remote sensing. Limnol. Oceanogr. **49:** 2179–2189.

———, L. Metsamaa, and A. G. Dekker. 2008. Influence of the vertical distribution of cyanobacteria in the water column on the remote sensing signal. Estuar. Coast. Shelf Sci. **78:** 649–654, doi:10.1016/j.ecss.2008.02.024

McQueen, D. J., and D. R. S. Lean. 1987. Influence of water temperature and nitrogen to phosphorus ratios on the dominance of blue-green in Lake St. George, Ontario. Can. J. Fish. Aquat. Sci. **44:** 598–604, doi:10.1139/f87-073

Millie, D. F., and others. 2008. Influence of environmental conditions on late-summer cyanobacterial abundance in Saginaw Bay, Lake Huron. Aquat. Ecosyst. Health Manag. **11:** 196–205, doi:10.1080/14634980802099604

———, and others. 2009. Late-summer phytoplankton in western Lake Erie (Laurentian Great Lakes): Bloom distributions, toxicity, and environmental influences. Aquat. Ecol. **43:** 915–934, doi:10.1007/s10452-009-9238-7

19395590, 2010, 5, Downloaded from https://aslopubs.onlinelibrary.wiley.com/doi/10.4319/lo.2010.55.5.2025 by Noaa Department Of Commerce, Wiley Online Library on [30/12/2024]. See the Terms and Conditions (https://onlinelibrary.wiley.com/terms-and-conditions) on Wiley Online Library for rules of use; OA articles are governed by the applicable Creative Commons License

MONTAGNER, F. 2001. Reference model for MERIS level 2 processing. European Space Agency, document No. PO-TN-MEL-GS-0026.

PAERL, H. W. 1988. Nuisance phytoplankton blooms in coastal, estuarine, and inland waters. Limnol. Oceanogr. **33:** 823–847, doi:10.4319/lo.1988.33.4_part_2.0823

———, AND J. HUISMAN. 2008. Blooms like it hot. Science **320:** 57–58, doi:10.1126/science.1155398

———, AND ———. 2009. Climate change: A catalyst for global expansion of harmful cyanobacterial blooms. Environ. Microbiol. Rep. **1:** 27–37, doi:10.1111/j.1758-2229.2008.00004.x

POPE, R. M., AND E. S. FRY. 1997. Absorption spectrum (380–700 nm) of pure water. II. Integrating cavity measurements. Appl. Optics **36:** 8710–8723, doi:10.1364/AO.36.008710

RAST, M., J. L. BEZY, AND S. BRUZZI. 1999. The ESA medium resolution imaging spectrometer MERIS: A review of the instrument and its mission. Int. J. Remote Sens. **20:** 1681–1702, doi:10.1080/014311699212416

REYNOLDS, C. S., AND G. H. M. JAWORSKI. 1978. Enumeration of natural *Microcystis* populations. Br. Phycol. J. **13:** 269–277, doi:10.1080/00071617800650331

RINTA-KANTO, J. M., E. A. KONOPKO, J. M. DEBRUYN, R. A. BOURBONNIERE, G. L. BOYER, AND S. W. WILHELM. 2009. Lake Erie *Microcystis*: Relationship between microcystin production, dynamics of genotypes and environmental parameters in a large lake. Harmful Algae **8:** 665–673, doi:10.1016/j.hal.2008.12.004

ROBARTS, R. D., AND T. ZOHARY. 1987. Temperature effects on photosynthetic capacity, respiration, and growth rates of bloom-forming cyanobacteria. N. Z. J. Mar. Freshw. Res. **21:** 391–399, doi:10.1080/00288330.1987.9516235

RUIZ-VERDÚ, A., S. G. H. SIMIS, C. DE HOYAS, H. J. GONS, AND R. PEÑA. 2008. An evaluation of algorithms for the remote sensing of cyanobacterial biomass. Remote Sens. Environ. **112:** 3996–4008, doi:10.1016/j.rse.2007.11.019

SCHOWENGERDT, R. A. 1997. Remote sensing models and methods for image processing. Second edition. Academic Press.

SELLNER, K. G. 1997. Physiology, ecology, and toxic properties of marine cyanobacteria blooms. Limnol. Oceanogr. **42:** 1089–1104, doi:10.4319/lo.1997.42.5_part_2.1089

SIMIS, S. G. H., S. W. M. PETERS, AND H. J. GONS. 2005. Remote sensing of the cyanobacteria pigment phycocyanin in turbid inland water. Limnol. Oceanogr. **50:** 237–245.

———, A. RUIZ-VERDU, J. A. DOMINGUEZ, R. PENA-MARTINEZ, S. W. M. PETERS, AND H. J. GONS. 2007. Influence of phytoplankton pigment composition on remote sensing of cyanobacterial biomass. Remote Sens. Environ. **106:** 414–427, doi:10.1016/j.rse.2006.09.008

STORY, M., AND R. G. CONGALTON. 1986. Accuracy assessment: A user's perspective. Photogram. Eng. Remote Sens. **52:** 397–399.

STUMPF, R. P., AND P. J. WERDELL. 2010. Adjustment of ocean color sensor calibration through multi-band statistics. Opt. Express **18:** 401–412, doi:10.1364/OE.18.000401

SUBRAMANIUM, A., R. R. HOOD, C. W. BROWN, E. J. CARPENTER, AND D. G. CAPONE. 2002. Detecting *Trichodesmium* blooms in SeaWiFS imagery. Deep-Sea Res. Part II **49:** 107–121, doi:10.1016/S0967-0645(01)00096-0

VANDERPLOEG, H. A., J. R. LIEBIG, W. W. CARMICHAEL, M. A. AGY, T. H. JOHENGEN, G. L. FAHNENSTIEL, AND T. F. NALEPA. 2001. Zebra mussel (*Dreissena polymorpha*) selective filtration promoted toxic microcystis blooms in Saginaw Bay (Lake Huron) and Lake Erie. Can. J. Fish. Aquat. Sci. **58:** 1208–1221, doi:10.1139/cjfas-58-6-1208

VINCENT, R. K., X. QUIN, R. M. L. MCKAY, J. MINER, K. CZAJKOWSKI, J. SAVINO, AND T. BRIDGEMAN. 2004. Phycocyanin detection from LANDSAT TM data for mapping cyanobacterial blooms in Lake Erie. Remote Sens. Environ. **89:** 381–392, doi:10.1016/j.rse.2003.10.014

WYNNE, T. T., R. P. STUMPF, AND A. G. RICHARDSON. 2006. Discerning resuspended chlorophyll concentrations from ocean color satellite imagery. Cont. Shelf Res. **26:** 2583–2597, doi:10.1016/j.csr.2006.08.003

———, ———, M. C. TOMLINSON, R. A. WARNER, P. A. TESTER, J. DYBLE, AND G. L. FAHNENSTIEL. 2008. Relating spectral shape to cyanobacterial blooms in the Laurentian Great Lakes. Int. J. Remote Sens. **29:** 3665–3672, doi:10.1080/01431160802007640

YACOBI, Y. Z., A. GITELSON, AND M. MAYO. 1995. Remote sensing of chlorophyll in Lake Kinnert using high-spectral-resolution radiometer and Landsat TM: Spectral features of reflectance and algorithm development. J. Plankton Res. **17:** 2155–2173, doi:10.1093/plankt/17.11.2155

Associate editor: Dariusz Stramski

Received: 16 February 2010
Accepted: 18 May 2010
Amended: 31 May 2010

19395590, 2010, 5, Downloaded from https://aslopubs.onlinelibrary.wiley.com/doi/10.4319/lo.2010.55.5.2025 by Noaa Department Of Commerce, Wiley Online Library on [30/12/2024]. See the Terms and Conditions (https://onlinelibrary.wiley.com/terms-and-conditions) on Wiley Online Library for rules of use; OA articles are governed by the applicable Creative Commons License